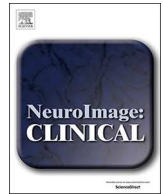




ELSEVIER

Contents lists available at ScienceDirect

NeuroImage: Clinical

journal homepage: www.elsevier.com/locate/ynicl

Disturbed neurovascular coupling in type 2 diabetes mellitus patients: Evidence from a comprehensive fMRI analysis



Bo Hu^{a,1}, Lin-Feng Yan^{a,1}, Qian Sun^{a,1}, Ying Yu^a, Jin Zhang^a, Yu-Jie Dai^b, Yang Yang^a, Yu-Chuan Hu^a, Hai-Yan Nan^a, Xin Zhang^a, Chun-Ni Heng^c, Jun-Feng Hou^c, Qing-Quan Liu^c, Chang-Hua Shao^d, Fei Li^d, Kai-Xiang Zhou^d, Hang Guo^d, Guang-Bin Cui^{a,*,2}, Wen Wang^{a,*,2}

^a Department of Radiology & Functional and Molecular Imaging Key Lab of Shaanxi Province, Tangdu Hospital, Fourth Military Medical University, 569 Xinsi Road, Xi'an 710038, Shaanxi, China

^b Department of Clinical Nutrition, Xijing Hospital, Fourth Military Medical University, 169 Changle Road, Xi'an 710032, Shaanxi, China

^c Department of Endocrinology, Tangdu Hospital, Fourth Military Medical University, 569 Xinsi Road, Xi'an 710038, Shaanxi Province, China

^d Student Brigade, Fourth Military Medical University, 169 Changle Road, Xi'an 710032, Shaanxi, China

ARTICLE INFO

Keywords:

Type 2 diabetes mellitus (T2DM)
Functional magnetic resonance imaging (fMRI)
Neurovascular coupling
Blood oxygenation level dependent (BOLD)
Arterial spin-labeling (ASL)
Cognitive impairment

ABSTRACT

Background: Previous studies presumed that the disturbed neurovascular coupling to be a critical risk factor of cognitive impairments in type 2 diabetes mellitus (T2DM), but distinct clinical manifestations were lacked. Consequently, we decided to investigate the neurovascular coupling in T2DM patients by exploring the MRI relationship between neuronal activity and the corresponding cerebral blood perfusion.

Methods: Degree centrality (DC) map and amplitude of low-frequency fluctuation (ALFF) map were used to represent neuronal activity. Cerebral blood flow (CBF) map was used to represent cerebral blood perfusion. Correlation coefficients were calculated to reflect the relationship between neuronal activity and cerebral blood perfusion.

Results: At the whole gray matter level, the manifestation of neurovascular coupling was investigated by using 4 neurovascular biomarkers. We compared these biomarkers and found no significant changes. However, at the brain region level, neurovascular biomarkers in T2DM patients were significantly decreased in 10 brain regions. ALFF-CBF in left hippocampus and fractional ALFF-CBF in left amygdala were positively associated with the executive function, while ALFF-CBF in right fusiform gyrus was negatively related to the executive function. The disease severity was negatively related to the memory and executive function. The longer duration of T2DM was related to the milder depression, which suggests T2DM-related depression may not be a physiological condition but be a psychological condition.

Conclusion: Correlations between neuronal activity and cerebral perfusion maps may be a method for detecting neurovascular coupling abnormalities, which could be used for diagnosis in the future.

Trial registry number: This study has been registered in [ClinicalTrials.gov](https://clinicaltrials.gov) (NCT02420470) on April 2, 2015 and published on July 29, 2015.

Abbreviations: T2DM, Type 2 diabetes mellitus; HC, healthy controls; BOLD, Blood Oxygenation Level Dependent; ASL, Arterial Spin-Labeling; CBF, Cerebral Blood Flow; DC, Degree Centrality; DCP, Positive Degree Centrality; DCN, Negative Degree Centrality; ALFF, Amplitude of Low-Frequency Fluctuation; fALFF, fractional Amplitude of Low-Frequency Fluctuation; HRF, Hemodynamic Response Function; GM, Gray Matter; FBG, Fasting Blood glucose; HbA_{1c}, Hemoglobin A_{1c}; PBG, Postprandial blood glucose; MMSE, Mini Mental State Examination; MoCA, Montreal Cognitive Assessment; SAS, Self-Rating Anxiety Scale; SDS, Self-Rating Depression Scale; CVLT, California Verbal-Learning Test; STROOP, Stroop Color Word Test; GSR, Global Signal Regression; FFG, Fusiform Gyrus; MFG, Middle Frontal Gyrus; MTG, Middle Frontal Gyrus Orbital Part; STG, Superior Temporal Gyrus; MTG, Middle Temporal Gyrus; MCPG, Median Cingulate and Paracingulate Gyri; LNP, Lenticular Nucleus Pallidum

* Corresponding authors at: Department of Radiology & Functional and Molecular Imaging Key Lab of Shaanxi Province, Tangdu Hospital, Fourth Military Medical University (Air Force Medical University), 569 Xinsi Road, Xi'an 710038, China.

E-mail addresses: wangwen@fmmu.edu.cn (W. Wang), cuibgt@fmmu.edu.cn (G.-B. Cui).

¹ These authors contributed equally.

² These authors are co-senior authors of the study.

<https://doi.org/10.1016/j.nicl.2019.101802>

Received 26 November 2018; Received in revised form 12 March 2019; Accepted 26 March 2019

Available online 27 March 2019

2213-1582/ © 2019 The Authors. Published by Elsevier Inc. This is an open access article under the CC BY-NC-ND license (<http://creativecommons.org/licenses/by-nc-nd/4.0/>).

1. Introduction

Type 2 diabetes mellitus (T2DM) has been proved to be a major risk factor for cognitive impairment, which may further progress to Alzheimer's disease (AD) or dementia (Biessels et al., 2008; Okereke et al., 2008; Roberts et al., 2014). Specific interventions are of great importance for treating it and preventing the progression, but personalized treatment is usually based on a clarified pathogenesis, which is still ambiguous (Cooper et al., 2015; Wang et al., 2016). Although microvascular disorders are supposed to be the major cause in previous studies, the process still can't be comprehensively explained (De Silva and Faraci, 2016; Hardigan et al., 2016).

Recently, several studies reported that the disturbed brain neurovascular coupling might be the underlying mechanism for cognitive impairment in T2DM (Goldin et al., 2006; Mogi and Horiuchi, 2011; Zhou et al., 2014a). In 2010, Attwell et al. suggested that neurons and blood vessels should be regarded as a functional complex, which is called the neurovascular unit (Attwell et al., 2010). This unit plays a pivotal role in maintaining the normal brain function by providing the sufficient blood to the corresponding neurons. However, the neurotoxic impact of advanced glycation end products (AGEs) could disturb this coupling, leading to a disproportionate blood supply (Brownlee, 2001; Vetri et al., 2017; Vetri et al., 2012). And this disturbance was usually referred to as a leading cause of cognitive impairment and even AD (Mogi and Horiuchi, 2011; Nicolakakis and Hamel, 2011; Rancillac et al., 2012; Rosengarten et al., 2009; Serlin et al., 2011; Tarantini et al., 2015). However, all these effects were observed on animal models, and more efforts are needed to investigate the condition of neurovascular coupling in T2DM patients.

Disrupted neurovascular coupling was reported in previous studies, but these studies based on only unimodal imaging techniques that reflecting either cerebral perfusion or neuronal activity, which could not comprehensively reflect their coupling (Duarte et al., 2015; Wong et al., 2016). Multimodal MRI is used to evaluate brain abnormalities in multiple aspects. Degree centrality (DC) map and amplitude of low-frequency fluctuation (ALFF) map derived from blood oxygenation level dependent (BOLD) signals can objectively reflect the regional neuronal activities (Biswal et al., 1995; Tomasi and Volkow, 2010; Zang et al., 2007). ALFF is measured by calculating the maximal fluctuation in low-frequency Hemodynamic Response Function (HRF) of each voxel, and the stronger fluctuation is usually regarded as the result of the stronger neural activity. DC is generally measured by extracting the time series of one voxel and correlating it with the time series of all the other voxels in the brain, and then calculating the summation of the resultant correlation coefficients. The higher DC usually means there are more correlations between this voxel and all the other voxels, which indicates that neurons in this voxel is more active. In addition, cerebral blood flow (CBF) map derived from arterial spin-labeling (ASL) signal is used to evaluate cerebral perfusion without introducing radiation exposure or exogenous contrast agent (Hendrikse et al., 2012; Pollock et al., 2009). Now that the condition of cerebral perfusion and neuronal activity of each voxel could be separately represented by aforementioned maps, the correlation between them could be analyzed to represent the neurovascular coupling. Besides, previous study suggested that the correlation between CBF and DC could effectively reflect this coupling in healthy subjects (Liang et al., 2013). Consequently, the condition of neurovascular coupling in T2DM patients could be investigated through this method.

This study will explore CBF-ALFF and CBF-DC correlation coefficients for reflecting neurovascular coupling in T2DM patients. In addition, while previous studies mostly investigated the neurovascular coupling at a whole gray matter (GM) level, which was quite ambiguous for precise treatment, we decided to further investigate it at brain region level. In the present study, we conducted a series of analyses to verify 3 hypotheses. First, the neuronal activity and cerebral perfusion were coupled under both physiological and diseased status. Second, the

neurovascular coupling in T2DM patients were disturbed at both whole GM level and brain region level. Finally, there was a potential relationship between brain function and the disease severity or imaging biomarkers.

2. Materials and methods

2.1. Participants

This study is a clinical trial and has been registered in [ClinicalTrials.gov \(NCT02420470\)](https://www.clinicaltrials.gov/ct2/show/study/NCT02420470). All experiments conformed to the principles of the Declaration of Helsinki and was approved by the ethics committee of Tangdu Hospital of Fourth Military Medical University. All participants provided informed written consent, and 95 T2DM patients and healthy controls were recruited from the endocrinology department of Tangdu hospital and the local community. All participants were right-handed and with a minimum of the high school education. Participants with fasting blood glucose (FBG) ≥ 7.0 mmol/L, and/or 2-hour blood glucose ≥ 11.1 mmol/L after an oral glucose tolerance test (OGTT) were considered to have diabetes. Healthy controls (HC) were characterized by fasting blood glucose < 6.1 mmol/L and 2-hour blood glucose < 7.8 mmol/L after OGTT. Subjects who met any one of the following conditions were excluded: other type of diabetes (type 1 diabetes or gestational diabetes), serious brain diseases (significant head trauma, tumor, stroke, meningitis), severe psychiatric illness (dementia, epilepsy, major depression), alcoholism or drug abuse, contraindication for MRI and severe visual or hearing loss. Six scans of the T2DM subjects and 5 scans of the HCs were excluded because of excessive motion (> 3 mm translation or $> 3^\circ$ rotation in any direction). Eight scans of the T2DM subjects and 4 scans were excluded because of large image artifacts. Five scans of the T2DM subjects and 6 scans were excluded because of incomplete scans or neuropsychological assessment. Finally, 31 T2DM patients and 30 HCs were recruited.

2.2. Clinical data and cognitive assessment

Clinical data were recorded, including age, sex, smoking and drinking habits, blood pressure (BP), body mass index (BMI), education levels and disease duration. FBG, hemoglobin A_{1c} (HbA_{1c}), urinary microalbumin, total cholesterol (TC), triglyceride, low-density lipoprotein cholesterol (LDL-C) and high-density lipoprotein cholesterol (HDL-C) were assessed at 8:00 A.M. after overnight fasting. Postprandial blood glucose (PBG) was assessed at 10:00 A.M. after drinking a 75 g glucose solution.

A series of cognitive assessments were completed, including the Mini Mental State Examination (MMSE), Montreal Cognitive Assessment (MoCA), Self-Rating Anxiety Scale (SAS), Self-Rating Depression Scale (SDS), California Verbal-Learning Test (CVLT) and Stroop Color Word Test (STROOP). Of these scales, MMSE was used to assess dementia and MoCA was used to screen participants with mild cognitive impairment (MCI) by assessing their general cognition. SAS was used to assess anxiety, and SDS was used to assess depression. CVLT included immediate and delayed recall tasks and was used to assess episodic memory for verbal information. STROOP was used to measure the selective attention and cognitive flexibility of the brain, in another word, executive function. All tests were conducted after the scan, and it took about 60 min for everyone to complete all the tests in a fixed order (MMSE, MoCA, CVLT, SAS, SDS, STROOP).

Statistical Package for the Social Sciences (SPSS) 20.0 (SPSS, Chicago, IL, USA) was used to analyze the socio-demographic and clinical data. Student *t*-test was used for analyzing quantitative data (age, body mass index, educational year, BP, FBG, PBG, urinary microalbumin, TC, triglyceride, LDL-C, HDL-C, SAS score, SDS score, MMSE score, MoCA score, STROOP score, and CVLT score), and the chi-square (χ^2) test was used for analyzing nominal qualitative data (gender, smoking and drinking habits).

2.3. MRI data acquisition

MRI data was acquired with a GE discovery MR750 3.0 T scanner (General Electric Medical Systems, USA) using an eight-channel phased-array head coil. Foam padding was used to restrict head movement and ear plugs were used to eliminate scanner noise. During the acquisition period, all participants were asked to keep their eyes closed and not to think anything. Structural images including high-resolution T1-weighted images were acquired by using a three-dimensional brain volume (3D-BRAVO) sequence, and functional images were acquired by using BOLD and ASL sequences. Detailed MRI settings were described in Supplementary material.

2.4. MRI data processing

The preprocessing procedure of BOLD signal included removing the first 10 time points, slice timing, realign, normalization, detrend, covariance regression and band-pass filtering. ALFF, fractional ALFF (fALFF), positive DC (DCP) and negative DC (DCN) maps were calculated, Z-score transformed and smoothed after preprocessing procedures. Note that ALFF and fALFF maps were calculated without the procedure of band-pass filtering, and DCN maps were calculated without global signal regression (GSR). For the ASL data, corresponding CBF images were obtained by using an automated image postprocessing tool in the ADW work station. The processing procedure of CBF maps included normalization, Z-score transformation and smoothing. Detailed processing procedures were described in Supplementary material.

2.5. Whole GM based neurovascular couplings and intergroup comparison

To quantitatively evaluate the neurovascular coupling, whole GM correlation was performed between images of neuronal activity (averaged ALFF, fALFF, DCP, DCN maps) and cerebral perfusion (averaged CBF maps). For each individual, 4 whole GM neurovascular biomarkers were assessed, i.e. ALFF-CBF, fALFF-CBF, DCP-CBF and DCN-CBF coefficients. Then these biomarkers were compared between T2DM and HC groups by using a two-tailed 2-sample student-t-test.

2.6. Brain region-based neurovascular coupling and intergroup comparison

To verify the uniformity of brain anatomy and function, the automated anatomical labeling (AAL) atlas was used to segregate the cerebrum into 90 independent regions (Tzourio-Mazoyer et al., 2002). The correlation coefficient between neuronal activity and cerebral perfusion was calculated for each brain region. Then these correlation coefficients were compared between T2DM and HC groups by using a two-tailed 2-sample student-t-test.

2.7. Correlation analysis between the brain function and disease severity or imaging biomarkers

All imaging characteristics and neuropsychological assessment with significant between-group differences found above were selected. A non-parametric Spearman's rank correlation analysis was conducted in this step to figure out the potential relationship between brain function and the disease severity as well as between brain function and neurovascular biomarkers.

2.8. Validation test

2.8.1. Voxel-wise perfusion/neuronal-activity ratio comparison

To evaluate the blood supply per unit of neuronal activity, we calculated the perfusion/neuronal-activity ratio for each voxel. Whole GM CBF/DCP, CBF/DCN, CBF/ALFF and CBF/fALFF ratio maps were computed. The intergroup differences of these ratio maps were tested in

a voxel-wise manner using a 2-sample student-t-test with age, sex, education levels and BMI as the nuisance variables. Multiple comparisons were corrected using a voxel-wise false discovery rate (FDR) method with a corrected threshold of $P < .05$. In addition, we also compared the CBF, DCP, DCN, ALFF, and fALFF maps between these 2 groups. Recently, the choice of multiple comparison correction method has been very controversial, because a weak method likely results in a false-positive result, while a strict method likely leads to a result difficult to replicate (Chen et al., 2018; Eklund et al., 2016). Consequently, we decided to explore the impact of multiple comparison correction method on the replicability of our study. Monte Carlo simulations (AlphaSim), Gaussian Random Field (GRF) theory correction, and permutation test were tried to see if different correction methods could influence the result.

2.8.2. The impact of GSR

Whether GSR should be conducted in the preprocessing procedure has been argued for a long time. Some researchers believe that GSR could remove physiological noise and signal fluctuation and improve the specificity of functional connectivity analysis (Fox et al., 2005; Weissenbacher et al., 2009). However, other researchers think that GSR could either introduce anti-correlations or alter interregional correlations, which may potentially spread underlying group differences to regions that may never have had (Fox et al., 2009; Saad et al., 2012). As a consequence, we decided to explore the impact of GSR on the replicability of our study.

3. Result

3.1. Demographic, clinical and neuropsychological results

No gray or white matter lesions were found in any participant according to FLAIR and T1-weighted images. The socio-demographic and clinical information for each group were presented in Table 1. No significant differences in age, gender, smoking or drinking habits, educational levels or BMI were observed between these 2 groups. Higher levels of FBG, PBG, HbA_{1c} and urinary microalbumin were found in T2DM group, but no significant differences in systolic and diastolic BP, triglyceride, TC, LDL-C or HDL-C were found. In terms of neuropsychological test (Table 2), no significant differences were found in MMSE, MoCA and their subitems. However, poorer performance was found in T2DM patients in 5 subitems of CVLT, i.e. Trial 4 ($P = .004$), Trial 5 ($P = .006$), Trial 1–5 ($P = .048$), Short Delay Free Recall ($P = .014$), and Short Delay Cued Recall ($P = .021$). Furthermore, poorer performance was found in T2DM patients in most subitems of STROOP, i.e. Correct ($P = .001$), Omission ($P = .006$), Congruent Correct (CC; $P = .006$), Congruent Reaction Time (CRT; $P = .026$), Incongruent Correct (IC; $P = .011$), Incongruent Reaction Time (IRT; $P = .006$), Pronunciation Relevant Correct (PRC; $P = .026$), Pronunciation Relevant Reaction Time (PRRT; $P = .002$), Irrelevant Correct (IRC; $P = .001$), and Irrelevant reaction time (IRRT; $P = .002$). In short, the memory and executive functions of T2DM patients were poorer than HCs.

3.2. Whole GM based neurovascular couplings and intergroup comparison

Averaged CBF, ALFF, fALFF, DCP and DCN maps of both T2DM and HC groups were showed in Fig. 1. No significant differences were found between these 2 groups (Fig. S1) in ALFF-CBF coefficient ($r_{DM} = 0.07 \pm 0.06$, $r_{HC} = 0.08 \pm 0.07$, $P = .377$), fALFF-CBF coefficient ($r_{DM} = 0.20 \pm 0.11$, $r_{HC} = 0.25 \pm 0.07$, $P = .052$), DCP-CBF coefficient ($r_{DM} = 0.14 \pm 0.10$, $r_{HC} = 0.13 \pm 0.11$, $P = .729$) and in DCN-CBF coefficient ($r_{DM} = -0.11 \pm 0.11$, $r_{HC} = -0.11 \pm 0.13$, $P = .992$). However, in fALFF-CBF coefficient, the P value was close to the threshold, which was different from the other 3 conditions.

Table 1
The socio-demographic and clinical information for these 2 groups.

	Type 2 diabetes (n = 31)	Healthy controls (n = 30)	P-value
Age (years)	51.39 ± 8.12	49.97 ± 6.20	0.197
Male/Female	24/7	18/12	0.174
BMI (kg/m ²)	25.49 ± 2.69	25.55 ± 1.58	0.917
Smoke (Never/Mild/Heavy)	19/5/6	20/4/7	0.906
Drink (Never/Mild/Heavy)	23/3/4	23/3/5	0.954
Education (years)	12.84 ± 2.75	12.97 ± 2.93	0.857
Systolic BP (mmHg)	126.50 ± 11.08	125.88 ± 12.36	0.836
Diastolic BP (mmHg)	79.17 ± 7.69	80.98 ± 10.19	0.435
Fasting glucose (mmol/L)	8.44 ± 3.45	6.48 ± 1.07	0.004*
Postprandial glucose (mmol/L)	11.7 ± 4.03	7.22 ± 0.54	< 0.001*
HbA _{1c} (%)	8.45 ± 3.45	6.48 ± 1.07	< 0.001*
Urinary microalbumin (µg/min)	49.32 ± 84.99	17.06 ± 13.26	0.044*
Duration of diabetes (months)	65.1 ± 53.8	–	–
Triglyceride (mmol/l)	2.45 ± 1.88	2.24 ± 1.24	0.611
Total cholesterol (mmol/l)	4.38 ± 1.28	4.09 ± 0.67	0.282
LDL-C (mmol/l)	2.62 ± 0.47	2.59 ± 0.52	0.817
HDL-C (mmol/l)	1.04 ± 0.31	0.96 ± 0.18	0.226

Data were reported as mean ± SD, and significant differences were labeled with asteroids. In smoking habit, mild < 20 cigarettes per day, and heavy ≥ 20 cigarettes per day. In drinking habit, mild < once a month, and heavy ≥ once a month.

3.3. Brain region-based neurovascular couplings and intergroup comparison

In ALFF-CBF coefficient (Fig. 2a), significant differences were found in left hippocampus ($r_{DM} = 0.65 \pm 0.20$, $r_{HC} = 0.74 \pm 0.12$, $P = .044$), left fusiform gyrus (FFG; $r_{DM} = 0.39 \pm 0.16$, $r_{HC} = 0.51 \pm 0.15$, $P = .003$), right FFG ($r_{DM} = 0.45 \pm 0.19$, $r_{HC} = 0.54 \pm 0.14$, $P = .034$) and right putamen ($r_{DM} = 0.87 \pm 0.09$, $r_{HC} = 0.90 \pm 0.04$, $P = .047$).

In DCN-CBF coefficient (Fig. 2b), significant differences were found in right MFGOP ($r_{DM} = 0.00 \pm 0.26$, $r_{HC} = -0.15 \pm 0.25$, $P = .026$) and right lenticular nucleus pallidum (LNP; $r_{DM} = 0.36 \pm 0.50$, $r_{HC} = 0.62 \pm 0.36$, $P = .022$).

In fALFF-CBF coefficient (Fig. 2c), significant differences were found in right middle frontal gyrus (MFG; $r_{DM} = 0.19 \pm 0.22$, $r_{HC} = 0.31 \pm 0.21$, $P = .039$), left middle frontal gyrus orbital part (MFGOP; $r_{DM} = -0.27 \pm 0.20$, $r_{HC} = -0.11 \pm 0.29$, $P = .022$), left amygdala ($r_{DM} = 0.47 \pm 0.39$, $r_{HC} = 0.66 \pm 0.26$, $P = .031$), left superior temporal gyrus (STG; $r_{DM} = 0.09 \pm 0.25$, $r_{HC} = 0.24 \pm 0.24$, $P = .027$) and right middle temporal gyrus (MTG; $r_{DM} = 0.17 \pm 0.18$, $r_{HC} = 0.27 \pm 0.14$, $P = .023$).

In DCP-CBF coefficient (Fig. 2d), significant differences were only found in right median cingulate and paracingulate gyri (MCPG; $r_{DM} = 0.27 \pm 0.21$, $r_{HC} = 0.13 \pm 0.21$, $P = .015$).

Briefly speaking, ALFF-CBF and fALFF-CBF in T2DM group were lower than HC group in left hippocampus, FFG, right putamen, right MFG, MFGOP, left amygdala, left STG and right MTG. DCN-CBF coefficients in right LNP was also lower in T2DM group, however, DCP-CBF coefficient in MCPG and DCN-CBF coefficient in MFGOP were significantly lower in HC group than T2DM group. The averaged correlation coefficients across all subjects and corresponding standard deviations were calculated and showed in Fig. 3. In addition, even the calculation method and distribution of signals of these 5 kinds of maps (ALFF, fALFF, DCP, DCN, and CBF) were different (Fig. 1), the distributions of brain region-based correlation coefficients were very similar (Fig. 4).

3.4. Correlation between brain function and the disease severity or imaging biomarkers

According to above experiments, SDS score, 10 STROOP subitems, and 5 CVLT subitems were selected to represent brain function. FBG, PBG, HbA_{1c}, and disease duration were selected to represent disease severity. Brain regions with significant imaging differences were selected to represent neurovascular coupling.

In terms of the relationship between brain function and disease severity (Fig. 5), PBG was negatively correlated with Trial 5 in CVLT (Spearman's $\rho = -0.566$, $P = .005$) and Trial 1–5 in CVLT (Spearman's $\rho = -0.485$, $P = .019$). HbA_{1c} was positively correlated with Omissions in STROOP (Spearman's $\rho = 0.455$, $P = .01$) and Trial 5 in CVLT (Spearman's $\rho = -0.385$, $P = .033$). And finally, the disease duration was negatively correlated with the SDS score (Spearman's $\rho = -0.471$, $P = .036$) and IC in STROOP (Spearman's $\rho = -0.53$, $P = .016$).

In terms of the relationship between brain function and neurovascular coupling (Fig. 6), ALFF-CBF coupling in left hippocampus was positively correlated with 5 STROOP subitems, i.e. Correct (Spearman's $\rho = 0.473$, $P = .007$), IC (Spearman's $\rho = 0.495$, $P = .005$), IRT (Spearman's $\rho = 0.440$, $P = .013$), PRC (Spearman's $\rho = 0.461$, $P = .009$), and PRRT (Spearman's $\rho = 0.427$, $P = .017$). In addition, ALFF-CBF coupling in right FFG was positively correlated with SDS score (Spearman's $\rho = 0.394$, $P = .028$) but negatively correlated with 3 STROOP subitems, i.e. IC (Spearman's $\rho = -0.382$, $P = .034$), PRC (Spearman's $\rho = -0.386$, $P = .032$), and PRRT (Spearman's $\rho = -0.370$, $P = .041$). Finally, fALFF-CBF coupling in left amygdala was positively correlated with 3 STROOP subitems, i.e. PRRT (Spearman's $\rho = 0.357$, $P = .049$), IC (Spearman's $\rho = 0.429$, $P = .016$), and IRT (Spearman's $\rho = 0.395$, $P = .028$).

As we can see, the consistent relationship between neuropsychological assessments and clinical indicators suggests that the brain function was negatively related to disease severity. The inconsistent relationships between neuropsychological assessments and neurovascular biomarkers indicates that relationships between brain function and neurovascular biomarkers depended on the coupling type and brain region.

3.5. Validation results

3.5.1. Voxel-wise perfusion/neuronal-activity ratio comparison

No significant differences were found in any map or ratio map through voxel-wise method, even several multiple comparison correction methods were tried.

3.5.2. The impact of GSR

ALFF, fALFF, and DCP maps were calculated without the GSR procedure and their correlations with CBF maps were reinvestigated (DCN maps were not included because GSR would result in negative correlations). Besides, the whole GM based and brain region-based comparisons were also conducted to see the extent to which GSR could influence the result. We found that GSR had slight influence on ALFF-CBF and fALFF-CBF couplings, but the influence on DCP-CBF coupling

Table 2
Neuropsychological assessments of T2DM group and HC group.

	Type 2 diabetes (n = 31)	Healthy controls (n = 30)	P-value
MMSE			
Total	28.23 ± 1.87	28.43 ± 1.13	0.605
Orientation	9.94 ± 0.25	9.86 ± 0.34	0.306
Registration	2.90 ± 0.40	2.99 ± 0.02	0.211
Attention and Calculation	4.23 ± 1.28	3.97 ± 1.61	0.489
Recall	2.35 ± 0.80	2.40 ± 0.66	0.792
Language and Praxis	8.84 ± 0.37	8.78 ± 0.48	0.602
MoCA			
Total	26.32 ± 2.43	25.63 ± 5.39	0.519
Executive Functions	0.71 ± 0.46	0.77 ± 0.40	0.563
Visuospatial Abilities	3.29 ± 0.86	3.19 ± 0.95	0.670
Naming Ability	3.00 ± 0	3.00 ± 0	1
Concentration	5.65 ± 0.71	5.60 ± 0.84	0.803
Language	2.77 ± 0.50	2.81 ± 0.53	0.771
Verbal abstraction	1.68 ± 0.48	60 ± 0.60	0.565
Recall	2.81 ± 1.54	3.52 ± 1.33	0.059
Orientation	5.96 ± 0.18	5.85 ± 0.57	0.311
CVLT			
Trial 1	4.76 ± 1.93	5.12 ± 1.87	0.461
Trial 2	7.83 ± 2.52	8.09 ± 2.20	0.667
Trial 3	9.01 ± 2.94	9.96 ± 2.81	0.202
Trial 4	9.56 ± 2.70	11.47 ± 2.18	0.004*
Trial 5	10.39 ± 3.43	12.56 ± 2.41	0.006*
Trial 1–5	41.56 ± 12.09	47.20 ± 9.54	0.048*
Short delay free recall	7.24 ± 2.94	9.17 ± 3.05	0.014*
Short delay cued recall	8.54 ± 2.26	9.95 ± 2.38	0.021*
Long delay free recall	8.15 ± 2.96	9.50 ± 2.81	0.074
Long delay cued recall	8.53 ± 2.70	9.61 ± 2.41	0.104
STROOP			
Correct	31.63 ± 10.48	45.17 ± 19.91	0.001*
Error	41.69 ± 7.64	36.63 ± 13.50	0.075
Omission	47.43 ± 9.82	38.86 ± 13.41	0.006*
Congruent Correct	4.88 ± 2.32	6.53 ± 3.58	0.037*
Congruent RT	191.67 ± 106.40	276.59 ± 176.46	0.026*
Incongruent Correct	14.09 ± 4.89	18.68 ± 8.38	0.011*
Incongruent RT	527.24 ± 243.23	795.67 ± 460.44	0.006*
Pronunciation	3.40 ± 1.83	5.10 ± 3.70	0.026*
Relevant Correct			
Pronunciation	134.27 ± 94.20	228.62 ± 195.87	0.002*
Relevant RT			
Irrelevant Correct	9.40 ± 4.49	15.02 ± 8.15	0.001*
Irrelevant RT	362.37 ± 222.61	647.84 ± 434.30	0.002*

Significant differences were labeled with asterisks. RT = Reaction time.

was severe. *P* values of ALFF-CBF, fALFF-CBF and DCP-CBF coupling were separately 0.353, 0.068 and 0.772, which were similar to those with GSR (Fig. S1 and Fig. S2). Brain region-based correlation coefficients were also recalculated and compared to those with GSR, and the influence of GSR on ALFF-CBF coupling and fALFF-CBF coupling was slight but on DCP-CBF coupling was severe (Fig. S3 for self-comparison and Fig. 7 for intergroup comparison).

4. Discussion

4.1. Main findings

At the whole GM level, the manifestation of neurovascular coupling was investigated by means of 4 neurovascular biomarkers, and we compared these biomarkers and found no significant changes. However, at the brain region level, neurovascular biomarkers in T2DM patients were significantly decreased in 10 brain regions and increased in 2 brain regions. ALFF-CBF in left hippocampus and fALFF-CBF in left amygdala were positively associated with the executive function, while ALFF-CBF in right fusiform gyrus was negatively related to the

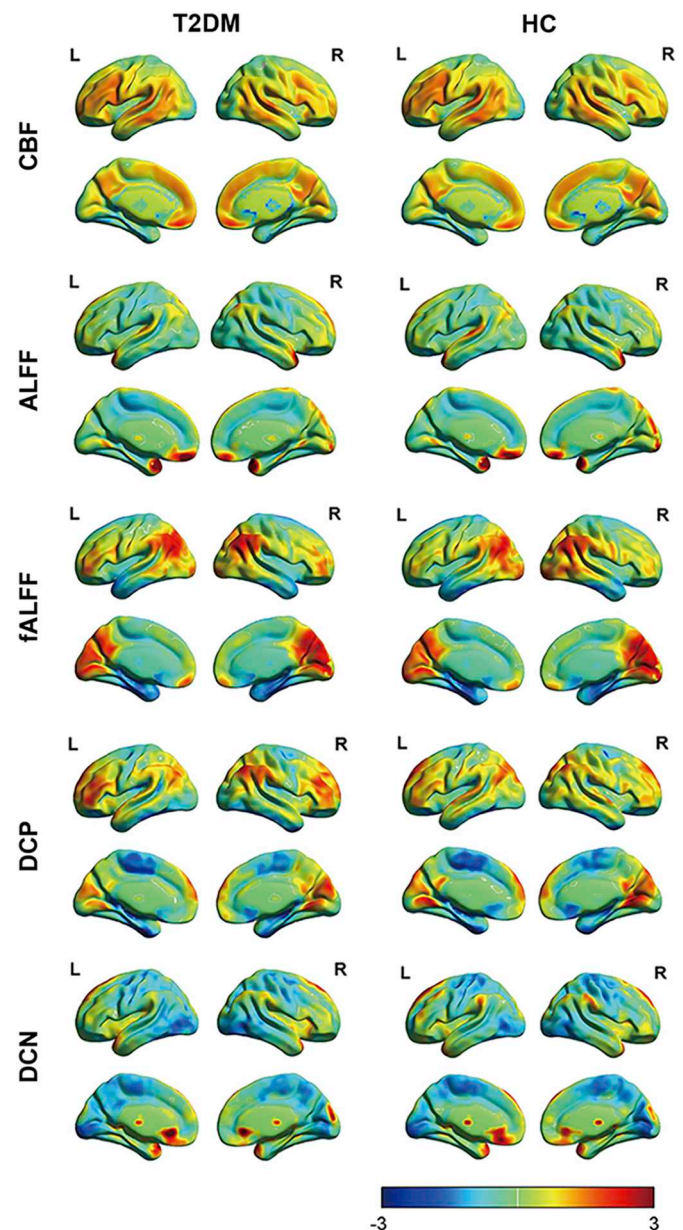


Fig. 1. Spatial distribution of averaged CBF, ALFF, fALFF, DCP and DCN maps. These maps were averaged across subjects within each group. T2DM = diabetes mellitus; HC = healthy control.

executive function.

The disease severity was negatively related to the STROOP reaction time, which indicates that patients with severe disease spend less time to think before action. The longer duration of T2DM is related to the milder depression, which suggests that T2DM-related depression may not be a physiological but psychological condition. In the future, neuropsychological assessments and neurovascular biomarkers could be combined for monitoring therapeutic efficacy and progression of cognitive impairment.

4.2. Relevant imaging studies

In 2013, Liang et al. introduced the whole GM based correlation between neuronal activity and cerebral perfusion maps, and this correlation was suggested as a imaging manifestation of neurovascular coupling (Liang et al., 2013). After that, Zhu et al. (Zhu et al., 2017) and Sheng et al. (Sheng et al., 2018) found the decreased coupling in

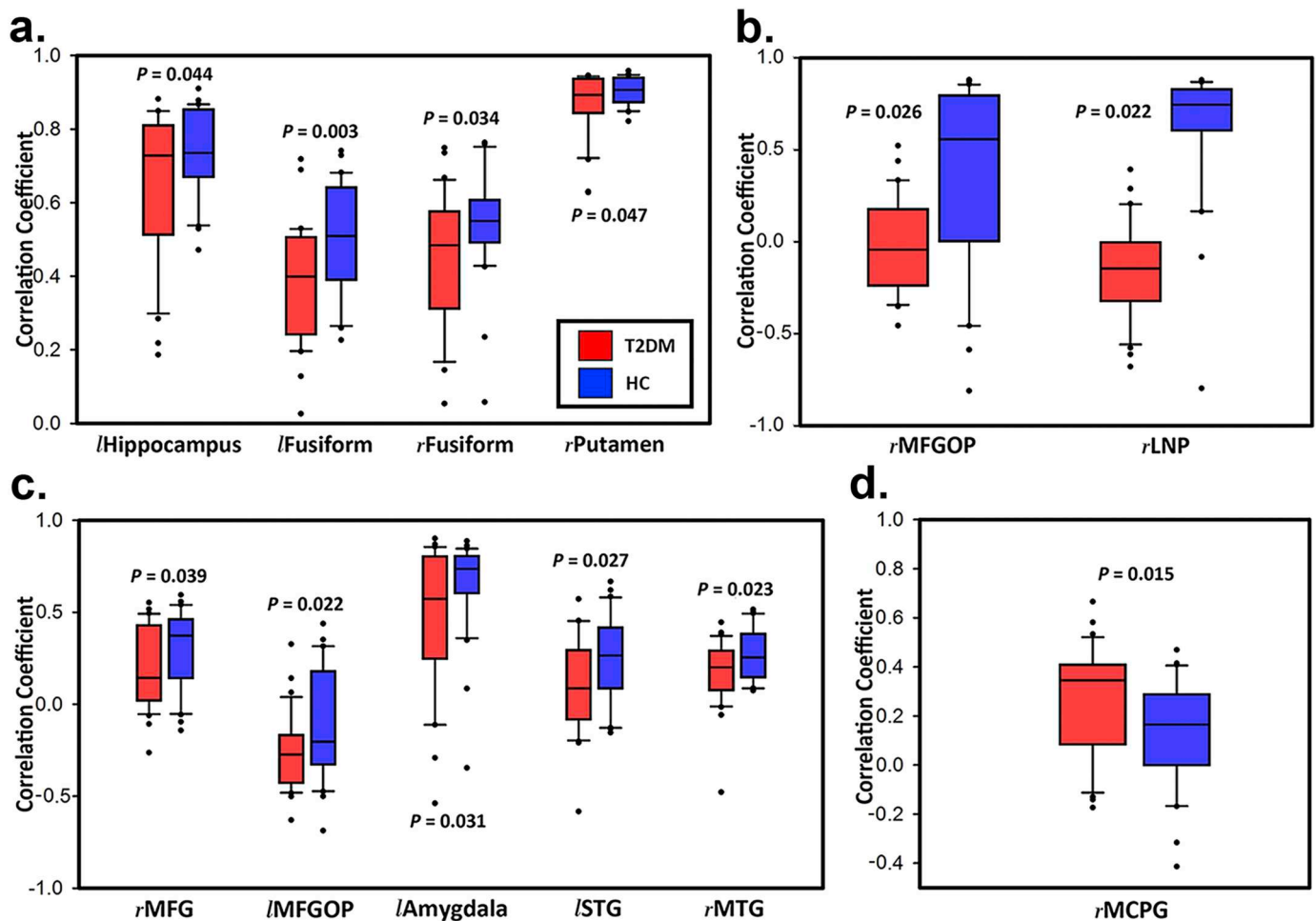


Fig. 2. Significant differences of 4 brain region-based neurovascular coupling biomarkers. (a) ALFF-CBF biomarker; (b) DCN-CBF biomarker; (c) fALFF-CBF biomarker; (d) DCP-CBF biomarker. *l* = left; *r* = right; MFGOP = middle frontal gyrus orbital part; LNP = lenticular nucleus pallidum; MFG = middle frontal gyrus; STG = superior temporal gyrus; MTG = middle temporal gyrus; MCPG = median cingulate and paracingulate gyri. Error bars represent the standard deviations and dots represent outliers.

schizophrenia and major depressive disorder. However, they analyzed only the correlation between CBF map and DCP map, while our findings are based on 4 different neurovascular biomarkers (ALFF-CBF, fALFF-CBF, DCP-CBF, DCN-CBF), which increases the credibility. The findings of decreased neurovascular coupling in T2DM patients should be instructive for the therapy of cognitive impairment in these people, because several medicines could be used to improve the neurovascular coupling condition (Munoz et al., 2015; Toth et al., 2014).

4.3. Potential physiological meanings

ALFF is defined as the total power within low frequency range (0.01 Hz ~ 0.1 Hz), while fALFF represents the relative contribution of specific low-frequency fluctuation to the whole frequency range. Usually, they were applied to the same sample group simultaneously to maximize reliability, but they are also used to detect unique characteristics (Zuo et al., 2010). Low-frequency oscillation are thought to reflect cyclic modulation of gross cortical excitability and long-distance neuronal synchronization (Balduzzi et al., 2008; Buzsaki and Draguhn, 2004). Zang et al. found that children with ADHD show reduced ALFF in some brain areas and increased amplitude in others compared with healthy controls (Zang et al., 2007). Yang et al. found gradual disturbances of ALFF and fALFF in Alzheimer Spectrum (Yang et al., 2018). Since the ALFF and fALFF maps were based on BOLD signal, they may reflect the oxygen uptake ability of neurons with above mentioned

function. Consequently, ALFF-CBF and fALFF-CBF may reflect the coordination between the requirement of oxygen and the blood supply, that is the function of neurovascular unit (Kisler et al., 2017).

DC is the summation of correlation coefficients between one voxel and all other voxels in the brain. Previous studies suggested that voxels with high DC are thought to serve as the interconnection brain hubs, which support fast communication with minimal energy cost (Tomasi and Volkow, 2010). Since the BOLD signal were acquired in resting state, DCP may represent the brain hubs for spontaneous brain activity, while DCN may represent the brain hubs in task state. As a result, DCP-CBF and DCN-CBF could be used to reflect the corresponding blood supply and metabolism of these brain hubs (Liang et al., 2013).

4.4. Brain regions and behavior

Brain regions with significant changes were different among these 4 biomarkers, including hippocampus, FFG, putamen, MFG, MFGOP, amygdala, STG, MTG, MCPG, and LNP. In addition, when we pre-process BOLD data without GSR, significantly lower neurovascular couplings were also found in olfactory and para hippocampal gyrus.

Hippocampus, para hippocampal gyrus, olfactory, amygdala and MCPG were the main components of the limbic system, which accounts for the brain memory function, sensory and emotion (Catani et al., 2013). Putamen, amygdala and LNP are components of basal ganglia and accounts for the regulation of movement (Andres and Darbin,

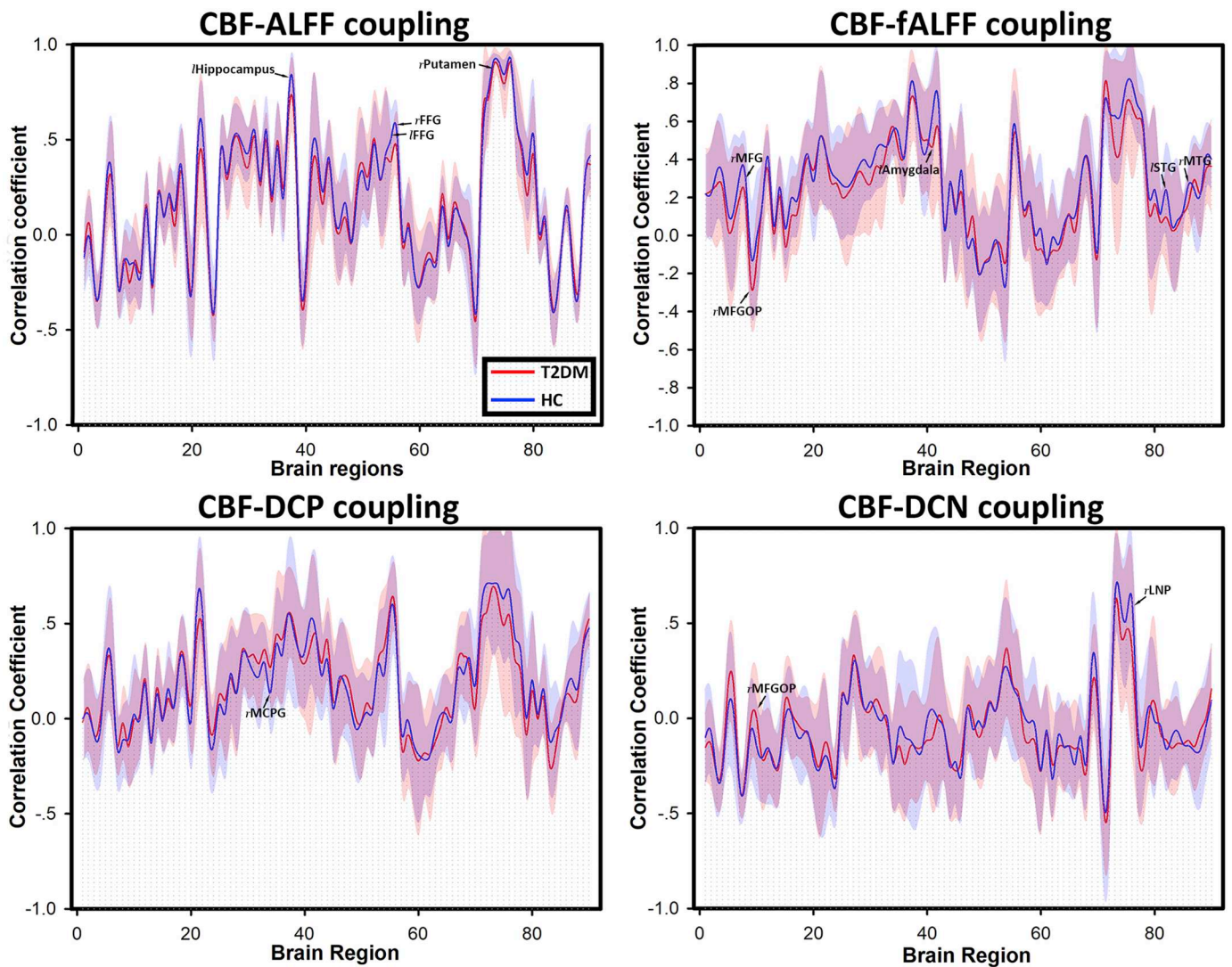


Fig. 3. Four kinds of brain region-based neurovascular coupling biomarkers. (a) ALFF-CBF biomarker; (b) fALFF-CBF biomarker; (c) DCP-CBF biomarker; (d) DCN-CBF biomarker. The numbers of brain regions were consistent with the numbers in Automated Anatomic labeling (AAL) atlas. Lines referred to the average correlation coefficients of brain regions within each group, and shadows of the corresponding color referred to the standard deviations. Brain regions with significant differences were labeled.

2018). MFG and MFGOP locate in the frontal lobe and accounts for the voluntary movement (Shibasaki, 2012). STG, MTG and FFG locate in the temporal lobe. Abnormalities in these brain regions may lead to the disruption of auditory processing, language comprehension or face recognition.

According to our findings, almost all brain regions showed significant lower neurovascular coupling in diabetic patients, except for DCP-CBF coefficient in MCPG and DCN-CBF coefficient in MFGOP, which aroused our interest. Previous study about MCPG is very few, because cingulate cortex is more often divided into anterior cingulate cortex (ACC) and posterior cingulate cortex (PCC). Prefrontal cortex, cingulate cortex and limbic system constitute the so-called Papez circuit, which controls the emotional expression, memory function and executive function (Aggleton et al., 2016). As far as we understand, the increasing neurovascular coupling in MCPG and MFGOP may result from a compensatory mechanism, because the limbic system is more damaged.

Neurovascular biomarkers were significantly related to 5 subitems of STROOP (Correct, IC, IRT, PRC and PRRT), and this scale mainly assesses the ability of executive function. “Correct” is the total correct number of the test, which indicates the overall executive function. “IC”

means the color of the test word is incongruent to the meaning, which indicates the inhibition function (Ben-David et al., 2011). “PRC” means the pronunciation of the test word is similar to the color, which indicates the parallel distributed processing function (Cohen et al., 1990). Our research suggests that in left hippocampus and amygdala, T2DM patients with lower neurovascular coupling tend to be more arbitrary in making decision, because their correct numbers were low while their reaction time is shorter. A meta-analysis also suggested that T2DM patients performs worse on STROOP test than healthy controls (Palta et al., 2014). However, in right FFG, ALFF-CBF is negatively related to brain functions and mental health (depression level). According to previous researches, FFG is involved in the processing of word and color information, which is coincident with the STROOP test (Hubbard and Ramachandran, 2005). The possible reason for the negative relationship is that the increased blood supply in T2DM patients is a compensatory effect.

4.5. Methodology enlightens

Previous studies have reported similar brain region abnormalities in T2DM, including hippocampal lesions (Hempel et al., 2012; Musen

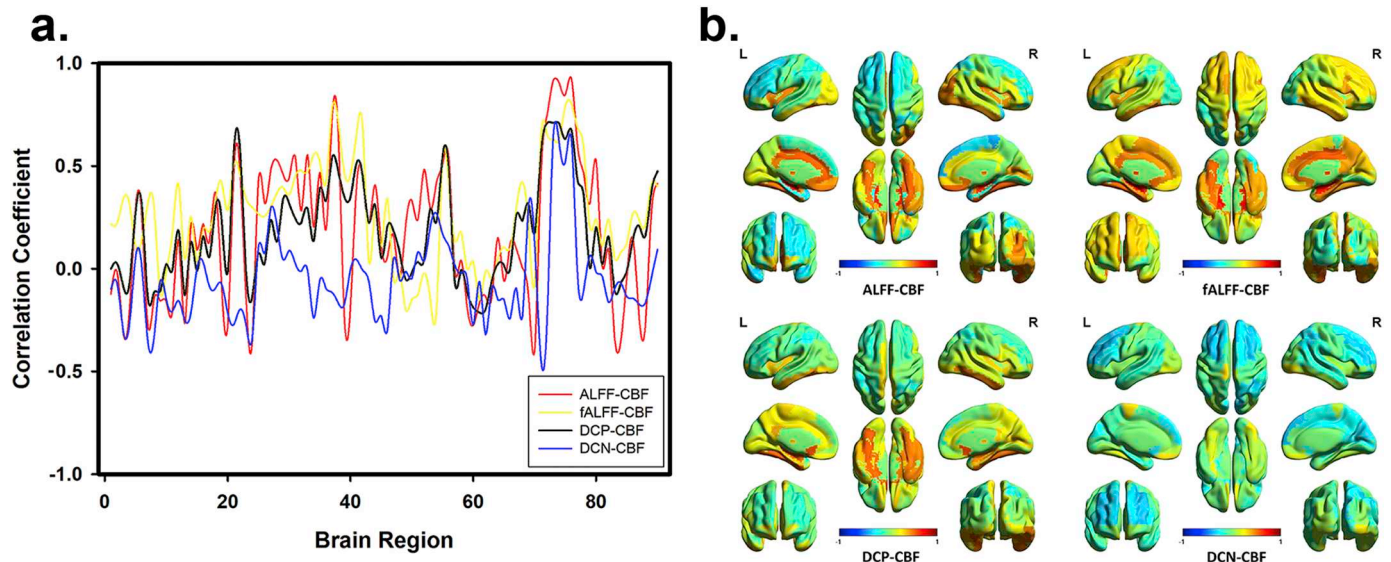


Fig. 4. The consistency of brain region-based correlation coefficients of different types. (a) Four kinds of neurovascular coupling biomarkers were calculated by using only parametric maps of HC group. Even the calculating methods of ALFF map, fALFF map, DCP map, and DCN map were totally different, the distribution and fluctuation of their brain region-based correlation coefficients with CBF map were similar. (b) The reconstructed brain maps of these 4 types of brain region-based correlation coefficients.

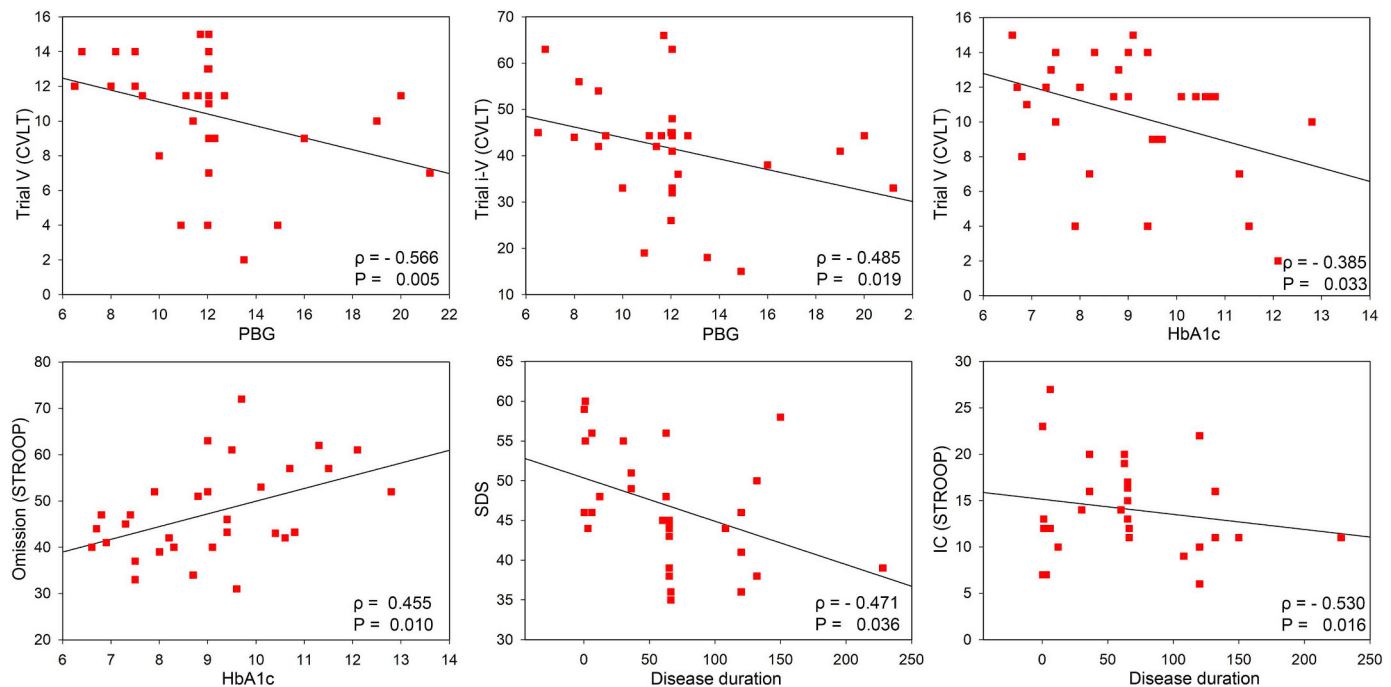


Fig. 5. Correlation analysis between brain function and disease severity. CVLT = California Verbal-Learning Test; Stroop = Stroop Color Word Test; SDS = Self-Rating Depression Scale; IC = Incongruent Correct; PBG = Postprandial Blood Glucose; HbA1c = hemoglobin A1c; Time = disease duration.

et al., 2012; Zhou et al., 2010), FFG and MTG lesions (Liu et al., 2016; Musen et al., 2012; Xia et al., 2013), and MFG, amygdala, cingulate and paracingulate gyrus lesions (Macpherson et al., 2017; Zhou et al., 2014b). However, we did not find any significant difference in voxel-wise analysis, even we had tried several methods for multiple comparison correction. This may indicate that voxel-wise method is not as sensitive as the coupling method we introduced for detecting brain lesions, or maybe the voxel-wise method is not suitable for detecting disturbed neurovascular couplings. In addition, the brain region-based coupling were quite stable between different groups of participants regardless of the small sample size, while the more reliable results of voxel-wise studies depends on a relative larger sample size (usually

upper than 40 participants per group)(Chen et al., 2018; Eklund et al., 2016).

4.6. Limitations

Although we tried to comprehensively clarify the neurovascular coupling in T2DM patients, there are still some limitations. First, the sample size is relatively small, which may influence the statistic power of our study. Second, ASL signals and BOLD signals were not acquired simultaneously. This defect may not have large influence on the result, because ALFF map and DC map were both time-independent. But future researches should focus on this issue to better unit the ASL signal and

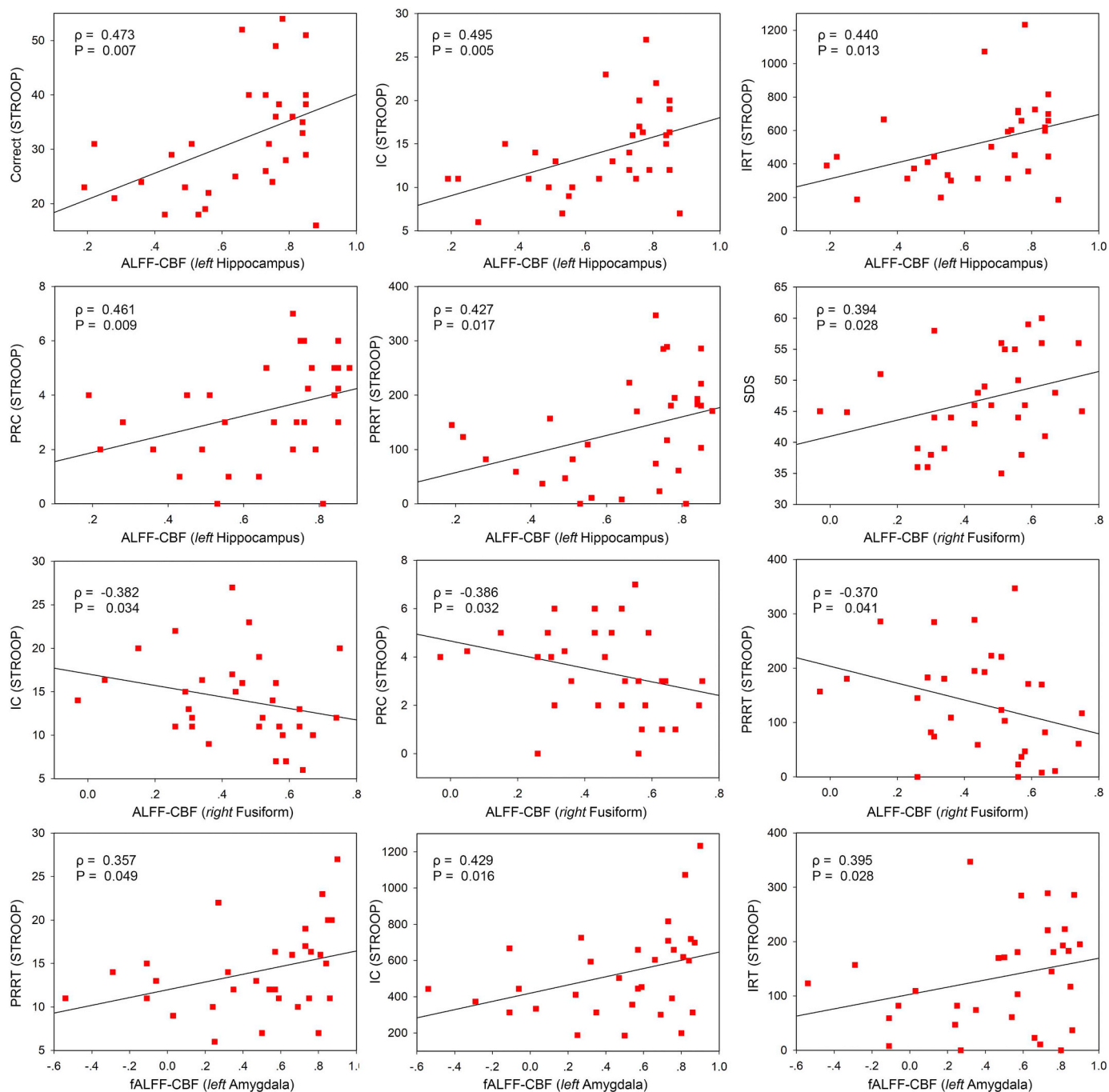


Fig. 6. Correlation analysis between brain function and neurovascular biomarkers. Stroop = Stroop Color Word Test; SDS = Self-Rating Depression Scale; IC = Incongruent Correct; IRT = Incongruent Reaction Time; PRC = Pronunciation Relevant Correct; PRRT = Pronunciation Relevant Reaction Time.

the BOLD signal to explain neurovascular coupling. Third, our findings were only based on imaging investigations, and future research could further verify our findings by uniting animal pathology and imaging. Fourth, our research is a cross-sectional study, so a longitudinal study is needed to explore the impact of treatments on the imaging biomarkers.

5. Conclusion

Correlations between neuronal activity and cerebral perfusion maps may be a method for detecting neurovascular coupling abnormalities, which could be used for diagnosis in the future.

Acknowledgements

The authors thank the clinical and the nursing team of the Endocrinology Department in Tangdu Hospital for their cooperation with work on involving participants. The authors thank Mr. Xiao-Cheng Wei (MR research, GE Healthcare China) for the excellent support.

Data availability

The datasets supporting the conclusions of this article are available in the [ClinicalTrials.gov](https://www.clinicaltrials.gov), [NCT02420470](https://www.clinicaltrials.gov/ct2/show/NCT02420470), <https://www.clinicaltrials.gov/ct2/show/NCT02420470?term=NCT02420470&rank=1>.

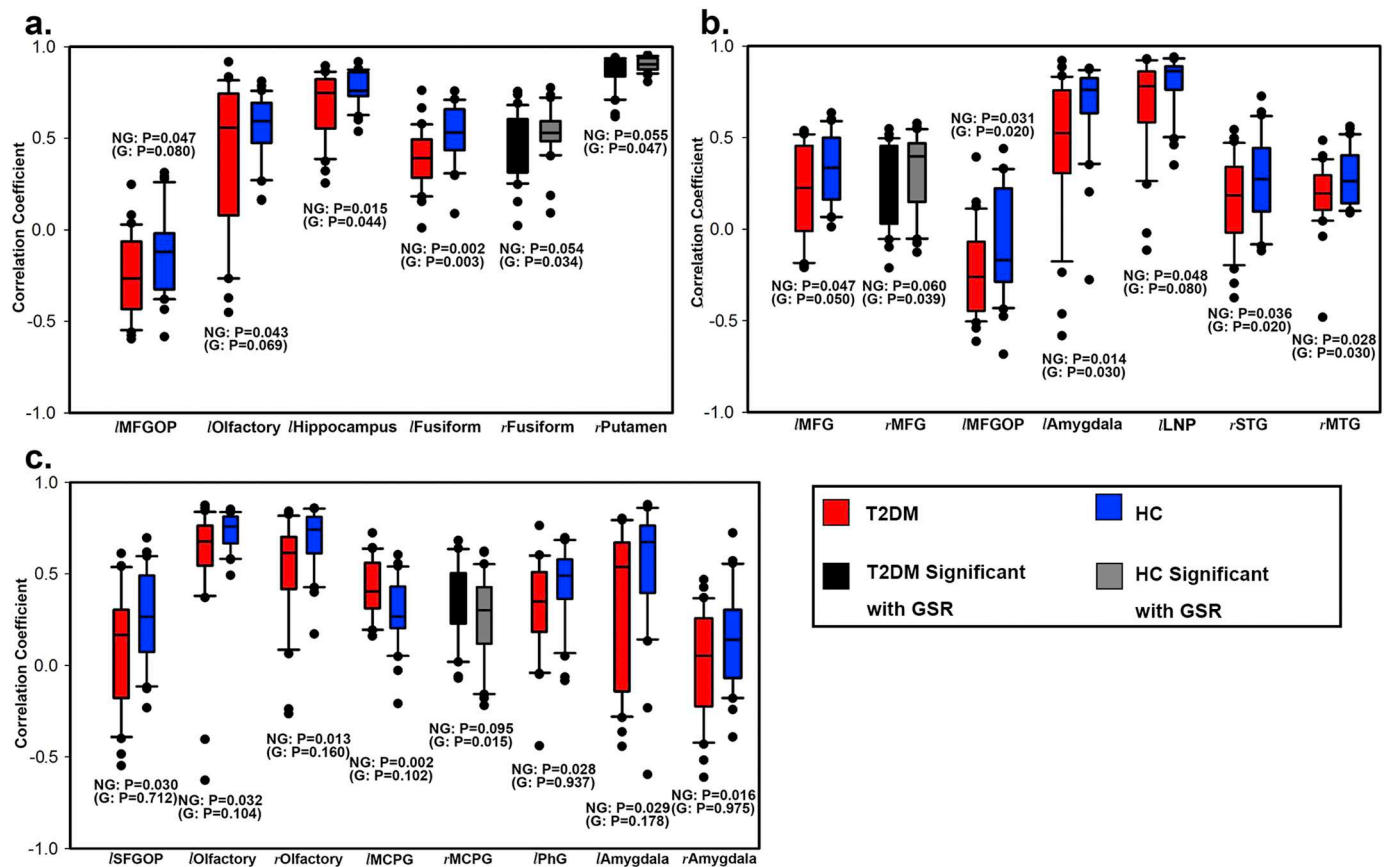


Fig. 7. Significant differences of 3 brain region-based neurovascular coupling biomarkers without GSR. (a) ALFF-CBF biomarker; (b) fALFF-CBF biomarker; (c) DCP-CBF biomarker. G = With GSR, NG = No GSR; l = left; r = right; MFGOP = middle frontal gyrus orbital part; MFG = middle frontal gyrus; STG = superior temporal gyrus; MTG = middle temporal gyrus; MCPG = median cingulate and paracingulate gyri; SFGOP = superior frontal gyrus orbital part; PhG = Para hippocampal gyrus. Error bars represent the standard deviations and dots represent outliers.

Competing interests

The authors declare that they have no competing interests.

Funding

This study received financial support from National Natural Science Foundation of China (No. 81471636 to Dr. Cui GB, No. 81771815 to Dr. Cui GB, No. 81801676 to Dr. Yu Y and No. 61603399 to Dr. Zhang X), Innovation and Development Foundation of Tangdu Hospital (No. 2016JCYJ002 to Dr. Yu Y). This study is also supported by Innovation and Development Foundation of Tangdu Hospital (No. 2017JSYJ006 to Dr. Sun Qian).

Appendix A. Supplementary data

Supplementary data to this article can be found online at <https://doi.org/10.1016/j.nicl.2019.101802>.

References

Aggleton, J.P., Pralus, A., Nelson, A.J., Hornberger, M., 2016. Thalamic pathology and memory loss in early Alzheimer's disease: moving the focus from the medial temporal lobe to Papez circuit. *Brain* 139, 1877–1890.
 Andres, D.S., Darbin, O., 2018. Complex dynamics in the basal ganglia: health and disease beyond the motor system. *J. Neuropsychiatr. Clin. Neurosci.* 30, 101–114.
 Attwell, D., Buchan, A.M., Chrapak, S., Lauritzen, M., Macvicar, B.A., Newman, E.A., 2010. Glial and neuronal control of brain blood flow. *Nature* 468, 232–243.
 Balduzzi, D., Riedner, B.A., Tononi, G., 2008. A BOLD window into brain waves. *Proc. Natl. Acad. Sci. U. S. A.* 105, 15641–15642.
 Ben-David, B.M., Nguyen, L.L., van Lieshout, P.H., 2011. Stroop effects in persons with

traumatic brain injury: selective attention, speed of processing, or color-naming? A meta-analysis. *J. Int. Neuropsychol. Soc.* 17, 354–363.
 Biessels, G.J., Deary, I.J., Ryan, C.M., 2008. Cognition and diabetes: a lifespan perspective. *Lancet Neurol.* 7, 184–190.
 Biswal, B., Yetkin, F.Z., Haughton, V.M., Hyde, J.S., 1995. Functional connectivity in the motor cortex of resting human brain using echo-planar MRI. *Magn. Reson. Med.* 34, 537–541.
 Brownlee, M., 2001. Biochemistry and molecular cell biology of diabetic complications. *Nature* 414, 813–820.
 Buzsaki, G., Draguhn, A., 2004. Neuronal oscillations in cortical networks. *Science* 304, 1926–1929.
 Catani, M., Dell'acqua, F., Thiebaut de Schotten, M., 2013. A revised limbic system model for memory, emotion and behaviour. *Neurosci. Biobehav. Rev.* 37, 1724–1737.
 Chen, X., Lu, B., Yan, C.G., 2018. Reproducibility of R-fMRI Metrics on the Impact of Different Strategies for Multiple Comparison Correction and Sample Sizes. vol. 39. pp. 300–318.
 Cohen, J.D., Dunbar, K., McClelland, J.L., 1990. On the control of automatic processes: a parallel distributed processing account of the Stroop effect. *Psychol. Rev.* 97, 332–361.
 Cooper, C., Sommerlad, A., Lyketsos, C.G., Livingston, G., 2015. Modifiable predictors of dementia in mild cognitive impairment: a systematic review and meta-analysis. *Am. J. Psychiatry* 172, 323–334.
 De Silva, T.M., Faraci, F.M., 2016. Microvascular dysfunction and cognitive impairment. *Cell. Mol. Neurobiol.* 36, 241–258.
 Duarte, J.V., Pereira, J.M., Quendera, B., Raimundo, M., Moreno, C., Gomes, L., Carrilho, F., Castelo-Branco, M., 2015. Early disrupted neurovascular coupling and changed event level hemodynamic response function in type 2 diabetes: an fMRI study. *J. Cereb. Blood Flow Metab.* 35, 1671–1680.
 Eklund, A., Nichols, T.E., Knutsson, H., 2016. Cluster failure: why fMRI inferences for spatial extent have inflated false-positive rates. *Proc. Natl. Acad. Sci. U. S. A.* 113, 7900–7905.
 Fox, M.D., Snyder, A.Z., Vincent, J.L., Corbetta, M., Van Essen, D.C., Raichle, M.E., 2005. The human brain is intrinsically organized into dynamic, anticorrelated functional networks. *Proc. Natl. Acad. Sci. U. S. A.* 102, 9673–9678.
 Fox, M.D., Zhang, D., Snyder, A.Z., Raichle, M.E., 2009. The global signal and observed anticorrelated resting state brain networks. *J. Neurophysiol.* 101, 3270–3283.
 Goldin, A., Beckman, J.A., Schmidt, A.M., Creager, M.A., 2006. Advanced glycation end products: sparking the development of diabetic vascular injury. *Circulation* 114,

- 597–605.
- Hardigan, T., Ward, R., Ergul, A., 2016. Cerebrovascular complications of diabetes: focus on cognitive dysfunction. *Clin. Sci. (Lond.)* 130, 1807–1822.
- Hempel, R., Onopa, R., Convit, A., 2012. Type 2 diabetes affects hippocampus volume differentially in men and women. *Diabetes Metab. Res. Rev.* 28, 76–83.
- Hendrikse, J., Petersen, E.T., Golay, X., 2012. Vascular disorders: insights from arterial spin labeling. *Neuroimaging Clin. N. Am.* 22 (259–269, x-xi).
- Hubbard, E.M., Ramachandran, V.S., 2005. Neurocognitive mechanisms of synesthesia. *Neuron* 48, 509–520.
- Kisler, K., Nelson, A.R., Rege, S.V., Ramanathan, A., Wang, Y., Ahuja, A., Lasic, D., Tsai, P.S., Zhao, Z., Zhou, Y., 2017. Pericyte degeneration leads to neurovascular uncoupling and limits oxygen supply to brain. vol. 20. pp. 406–416.
- Liang, X., Zou, Q., He, Y., Yang, Y., 2013. Coupling of functional connectivity and regional cerebral blood flow reveals a physiological basis for network hubs of the human brain. *Proc. Natl. Acad. Sci. U. S. A.* 110, 1929–1934.
- Liu, D., Duan, S., Zhang, J., Zhou, C., Liang, M., Yin, X., Wei, P., Wang, J., 2016. Aberrant brain regional homogeneity and functional connectivity in middle-aged T2DM patients: a resting-state functional MRI study. *Front. Hum. Neurosci.* 10, 490.
- Macpherson, H., Formica, M., Harris, E., Daly, R.M., 2017. Brain functional alterations in type 2 diabetes - a systematic review of fMRI studies. *Front. Neuroendocrinol.* 47, 34–46.
- Mogi, M., Horiuchi, M., 2011. Neurovascular coupling in cognitive impairment associated with diabetes mellitus. *Circ. J.* 75, 1042–1048.
- Munoz, M.F., Puebla, M., Figueroa, X.F., 2015. Control of the neurovascular coupling by nitric oxide-dependent regulation of astrocytic Ca(2+) signaling. *Front. Cell. Neurosci.* 9, 59.
- Musen, G., Jacobson, A.M., Bolo, N.R., Simonson, D.C., Shenton, M.E., McCartney, R.L., Flores, V.L., Hoogenboom, W.S., 2012. Resting-state brain functional connectivity is altered in type 2 diabetes. *Diabetes* 61, 2375–2379.
- Nicolakakis, N., Hamel, E., 2011. Neurovascular function in Alzheimer's disease patients and experimental models. *J. Cereb. Blood Flow Metab.* 31, 1354–1370.
- Okereke, O.I., Kang, J.H., Cook, N.R., Gaziano, J.M., Manson, J.E., Buring, J.E., Grodstein, F., 2008. Type 2 diabetes mellitus and cognitive decline in two large cohorts of community-dwelling older adults. *J. Am. Geriatr. Soc.* 56, 1028–1036.
- Palta, P., Schneider, A.L., Biessels, G.J., Touradjji, P., Hill-Briggs, F., 2014. Magnitude of cognitive dysfunction in adults with type 2 diabetes: a meta-analysis of six cognitive domains and the most frequently reported neuropsychological tests within domains. *J. Int. Neuropsychol. Soc.* 20, 278–291.
- Pollock, J.M., Tan, H., Kraft, R.A., Whitlow, C.T., Burdette, J.H., Maldjian, J.A., 2009. Arterial spin-labeled MR perfusion imaging: clinical applications. *Magn. Reson. Imaging Clin. N. Am.* 17, 315–338.
- Rancillac, A., Geoffroy, H., Rossier, J., 2012. Impaired neurovascular coupling in the APPxPS1 mouse model of Alzheimer's disease. *Curr. Alzheimer Res.* 9, 1221–1230.
- Roberts, R.O., Knopman, D.S., Geda, Y.E., Cha, R.H., Pankratz, V.S., Baerlein, L., Boeve, B.F., Tangalos, E.G., Ivnik, R.J., Mielke, M.M., Petersen, R.C., 2014. Association of diabetes with amnesic and nonamnesic mild cognitive impairment. *Alzheimers Dement.* 10, 18–26.
- Rosengarten, B., Paulsen, S., Burr, O., Kaps, M., 2009. Neurovascular coupling in Alzheimer patients: effect of acetylcholine-esterase inhibitors. *Neurobiol. Aging* 30, 1918–1923.
- Saad, Z.S., Gotts, S.J., Murphy, K., Chen, G., Jo, H.J., Martin, A., Cox, R.W., 2012. Trouble at rest: how correlation patterns and group differences become distorted after global signal regression. *Brain Connect.* 2, 25–32.
- Serlin, Y., Levy, J., Shalev, H., 2011. Vascular pathology and blood-brain barrier disruption in cognitive and psychiatric complications of type 2 diabetes mellitus. *Cardiovasc. Psychiatry Neurol.* 2011, 609202.
- Sheng, J., Shen, Y., Qin, Y., Zhang, L., Jiang, B., Li, Y., Xu, L., Chen, W., Wang, J., 2018. Spatiotemporal, metabolic, and therapeutic characterization of altered functional connectivity in major depressive disorder. vol. 39. pp. 1957–1971.
- Shibasaki, H., 2012. Cortical activities associated with voluntary movements and involuntary movements. *Clin. Neurophysiol.* 123, 229–243.
- Tarantini, S., Hertelendy, P., Tucsek, Z., Valcarcel-Ares, M.N., Smith, N., Menyhart, A., Farkas, E., Hodges, E.L., Townner, R., Deak, F., Sonntag, W.E., Csiszar, A., Ungvari, Z., Toth, P., 2015. Pharmacologically-induced neurovascular uncoupling is associated with cognitive impairment in mice. *J. Cereb. Blood Flow Metab.* 35, 1871–1881.
- Tomasi, D., Volkow, N.D., 2010. Functional connectivity density mapping. *Proc. Natl. Acad. Sci. U. S. A.* 107, 9885–9890.
- Toth, P., Tarantini, S., Tucsek, Z., Ashpole, N.M., Sosnowska, D., Gautam, T., Ballabh, P., Koller, A., Sonntag, W.E., Csiszar, A., Ungvari, Z., 2014. Resveratrol treatment rescues neurovascular coupling in aged mice: role of improved cerebrovascular endothelial function and downregulation of NADPH oxidase. *Am. J. Physiol. Heart Circ. Physiol.* 306, H299–H308.
- Tzourio-Mazoyer, N., Landeau, B., Papathanassiou, D., Crivello, F., Etard, O., Delcroix, N., Mazoyer, B., Joliot, M., 2002. Automated anatomical labeling of activations in SPM using a macroscopic anatomical parcellation of the MNI MRI single-subject brain. *Neuroimage* 15, 273–289.
- Vetri, F., Xu, H., Paisansathan, C., Pelligrino, D.A., 2012. Impairment of neurovascular coupling in type 1 diabetes mellitus in rats is linked to PKC modulation of BK(Ca) and Kir channels. *Am. J. Physiol. Heart Circ. Physiol.* 302, H1274–H1284.
- Vetri, F., Qi, M., Xu, H., Oberholzer, J., Paisansathan, C., 2017. Impairment of neurovascular coupling in Type 1 Diabetes Mellitus in rats is prevented by pancreatic islet transplantation and reversed by a semi-selective PKC inhibitor. *Brain Res.* 1655, 48–54.
- Wang, Y.F., Ji, X.M., Lu, G.M., Zhang, L.J., 2016. Resting-state functional MR imaging shed insights into the brain of diabetes. *Metab. Brain Dis.* 31, 993–1002.
- Weissenbacher, A., Kasess, C., Gerstl, F., Lanzenberger, R., Moser, E., Windischberger, C., 2009. Correlations and anticorrelations in resting-state functional connectivity MRI: a quantitative comparison of preprocessing strategies. *Neuroimage* 47, 1408–1416.
- Wong, R.H., Raedersdorff, D., Howe, P.R., 2016. Acute resveratrol consumption improves neurovascular coupling capacity in adults with type 2 diabetes mellitus. *Nutrients* 8.
- Xia, W., Wang, S., Sun, Z., Bai, F., Zhou, Y., Yang, Y., Wang, P., Huang, Y., Yuan, Y., 2013. Altered baseline brain activity in type 2 diabetes: a resting-state fMRI study. *Psychoneuroendocrinology* 38, 2493–2501.
- Yang, L., Yan, Y., Wang, Y., Hu, X., Lu, J., Chan, P., Yan, T., Han, Y., 2018. Gradual disturbances of the amplitude of low-frequency fluctuations (ALFF) and fractional ALFF in Alzheimer spectrum. *Front. Neurosci.* 12, 975.
- Zang, Y.F., He, Y., Zhu, C.Z., Cao, Q.J., Sui, M.Q., Liang, M., Tian, L.X., Jiang, T.Z., Wang, Y.F., 2007. Altered baseline brain activity in children with ADHD revealed by resting-state functional MRI. *Brain Dev.* 29, 83–91.
- Zhou, H., Lu, W., Shi, Y., Bai, F., Chang, J., Yuan, Y., Teng, G., Zhang, Z., 2010. Impairments in cognition and resting-state connectivity of the hippocampus in elderly subjects with type 2 diabetes. *Neurosci. Lett.* 473, 5–10.
- Zhou, H., Zhang, X., Lu, J., 2014a. Progress on diabetic cerebrovascular diseases. *Bosn. J. Basic Med. Sci.* 14, 185–190.
- Zhou, X., Zhang, J., Chen, Y., Ma, T., Wang, Y., Wang, J., Zhang, Z., 2014b. Aggravated cognitive and brain functional impairment in mild cognitive impairment patients with type 2 diabetes: a resting-state functional MRI study. *J. Alzheimers Dis.* 41, 925–935.
- Zhu, J., Zhuo, C., Xu, L., Liu, F., Qin, W., Yu, C., 2017. Altered coupling between resting-state cerebral blood flow and functional connectivity in schizophrenia. *Schizophr. Bull.* 43, 1363–1374.
- Zuo, X.N., Di Martino, A., Kelly, C., Shehzad, Z.E., Gee, D.G., Klein, D.F., Castellanos, F.X., Biswal, B.B., Milham, M.P., 2010. The oscillating brain: complex and reliable. *Neuroimage* 49, 1432–1445.